

## Phase and Mechanical Properties Response of the Mechanically Alloyed CoCrFeNiAlX High Entropy Alloys

Angelina Strakosova (0000-0002-1276-7263)\*, Petr Kratochvíl (0000-0002-1720-4646), Jan Riedl (0000-0003-4633-3073), Filip Průša (0000-0002-6494-5084)

Department of Metals and Corrosion Engineering, University of Chemistry and Technology Prague. Technická 5, 166 28 Prague 6. Czech Republic. E-mail: \*strakosn@vscht.cz

The present work describes the influence of Al content on the CoCrFeNiAl high-entropy alloys prepared by the powder metallurgy technique. The preparation procedure consisted of mechanical alloying and subsequent spark plasma sintering. The content of Al varied from 10 – 30 at.% which affected the microstructure and mechanical properties. Using scanning electron microscope (SEM) and X-ray diffraction analysis (XRD) was found the microstructure becomes more grain refined with increasing content of Al accompanied by the annihilation of the ductile FCC solid solution ( $\text{Cr}_{0.25}\text{Fe}_{0.25}\text{Co}_{0.25}\text{Ni}_{0.25}$ ) phase and growth of the brittle and hard BCC solid solution phase ( $\alpha\text{-Fe}$ ) and formation of  $\text{Al}(\text{Co}_{0.5}\text{Ni}_{0.5})$  phases, improving the mechanical properties. The best combination of the porosity, hardness HV 30, and ultimate compressive strength (UCS) was achieved for the studied high-entropy alloy when it contained 20 at. % Al.

**Keywords:** High-Entropy Alloy, Mechanical Alloying, Spark Plasma Sintering, Mechanical Properties, Microstructure

### 1 Introduction

High-entropy alloys (HEA) are a new group of materials that arouses great interest in researching their structure and properties. Their study began in 2004 when the first scientific works were published [1,2]. HEAs are defined as alloys that consist of five or more chemical elements with a molar proportion of elements ranging from 5 % up to 35 %. Other elements with a content of less than 5% may be added further modifying the properties of these alloys [3-6]. Considering the fact, that the alloys consist of various elements with different percentage representations and foremostly wide range of melting temperatures, there are many techniques used for their preparation. Usually, they are prepared by arc melting [5], vacuum induction melting [7], physical vapour deposition [6], or mechanical alloying (MA) which is accompanied by subsequential compaction via spark plasma sintering (SPS) or hot isostatic pressing (HIP) [8].

Mechanical alloying is a representative of powder metallurgy processes. This technique uses repeated cold welding and splitting of powder particles in a high-energy ball mill [5,9]. The disadvantage of the process is the contamination of the prepared powder alloys from two different sources. The first of them can be the process control agent itself which is used to decrease the excessive cold welding or the material to the grinding elements and the vessel itself. The second source is the contamination with the material of the milling balls/jar which is easily induced due to the overall high hardness of many HEAs. The advantage

is the economy and simplicity of the MA process allowing the formation of homogeneous structures without segregation of elements, and the possibility to create new alloys, e.g. consisted of immiscible elements or with chemical compositions that could not be achieved by conventional casting techniques [10]. The prepared powder alloys are then compacted foremostly by methods that suppress the deleterious microstructural coarsening. The most commonly used is SPS technology which consists of rapid heating due to Joule heat within the metallic sample and of subsequential compression and sufficient dwell time on the compaction temperature, usually in a matter of minutes [8].

There are some studies focused on high-entropy CoCrFeNiAlX alloys [11-17] among which only a few are describing the influence of the Al addition on the microstructure and mechanical properties [11-13]. All of them are described as high-entropy alloys prepared by casting, vacuum induction, or arc melting technologies. The majority of these scientific works are focused on the study of the properties which are affected by elevated temperatures [15,16]. It was reported in the studies [11,15,16] that the higher the Al content the more grain refined microstructure. However, not only the microstructural appearance, but also the phase composition changes accordingly to W.R. Wang et al. [15] who reported the change of volume fraction of soft and ductile face-centered cubic (FCC) towards hard, but brittle body-centered cubic (BCC) solid solution. This was also confirmed by T. Yang et al. [12] describing the same trend by the

change in hardness. M.M. Garlapati et al. [17] studied the thermal stability of the AlXCoCrFeNi high-entropy alloy as a consequence of the Al content. Using the X-ray diffraction analysis, they described the decreasing intensity of the FCC solid solution peak and the transformation of it into the BCC solid solution phase as the thermal treatment temperature increases. In this work, the high-entropy alloy CoCrFeNiAlX with different Al content (X= 10, 20, 30 at. %), was prepared by mechanical alloying and compacted using a spark plasma sintering process. The prepared alloys were investigated to describe the influence of Al content in terms of phase composition, microstructure, and mechanical properties.

## 2 Material and methods

In the study the high-entropy CoFeCrNiAl powder alloys with Al content of 10, 20, and 30 at. %

**Tab. 1** *Weights of individual elements used for the preparation of the CoCrFeNiAl alloys*

	theoretical weight, g				
	Co	Cr	Fe	Ni	Al
Al10	4.964	4.380	4.704	4.944	1.010
Al20	4.668	4.120	4.424	4.650	2.136
Al30	4.338	3.828	4.110	4.320	3.404

Morphology of MA-prepared powders and microstructure were studied using a scanning electron microscope (SEM, Tescan Lyra equipped by EDS, 80 mm<sup>2</sup>). The samples for the microstructure characterization were prepared by grinding on abrasive papers with a grit size P 220-2500, polishing on diamond paste D2 and etching using an aqua regia solution. Relative surface porosity was measured on the images of polished alloys obtained from a light microscope Nikon ECLIPSE MA200 using a threshold method in the program ImageJ. The XRF (Thermo ARL 9400 XP) and the XRD analyses (X-ray diffractometer PANalytical X'Pert Pro) were used to determine the chemical and phase composition of the CoFeCrNiAlX alloys, respective. In terms of mechanical properties, the hardness HV 30 was measured within the direction of SPS compaction. Also, the compressive stress-strain tests of each studied alloy were made at room temperature using LabTest 5.250SP1-VM universal testing machine. For this reason, cubical-like samples were used with a strain speed of 0.001 s<sup>-1</sup>.

(hereinafter referred to as Al10, Al20, and Al30) were prepared by the mechanical alloying (MA) method within a planetary ball-milling device Retsch PM100. The parameters of the MA process were: 400 rpm and a total process duration of 8h. The amounts of individual elements are shown in Table 1. In each case, 4 wt.% of the n-heptane was added as a process control agent decreasing the excessive cold-welding of the powder to the inner parts of the milling jar. The next step was the compaction of prepared powder alloys via Spark Plasma Sintering (SPS) technology. For this purpose, the FCT Systeme HP-D 10 machine was used. The samples were heated with a heating rate of 200 °C/min up to 1000 °C and then compressed with a compaction pressure of 48 MPa. The sample remained compressed at 1000 °C for another 9 min and then was cooled down with the maximal cooling speed of the machine.

## 3 Results and discussions

### 3.1 Microstructure characterization

Figure 1 shows the change in the CoCrFeNiAlX powder morphology after 8 h of mechanical alloying as a result of increasing Al content. It is visible that the alloy powder is having an irregular shape, mostly composed of sharp-edged particles whose average dimension decreases with increasing content of Al. This is demonstrated in the Al10 alloy (Fig. 1a) having the biggest particles. On the contrary, the alloy with the highest Al content (Fig. 1c) has the finest powder with a particle size in the range of tens of micrometers. The decrease of the particle size is affected by the increasing content of the brittle BCC solid solution within the structure of such alloy. Unlike the ductile and soft FCC phase, which supports the formation of bulky powder particles, the BCC phase causes splitting into smaller-sized particles refining the overall appearance of the powder.

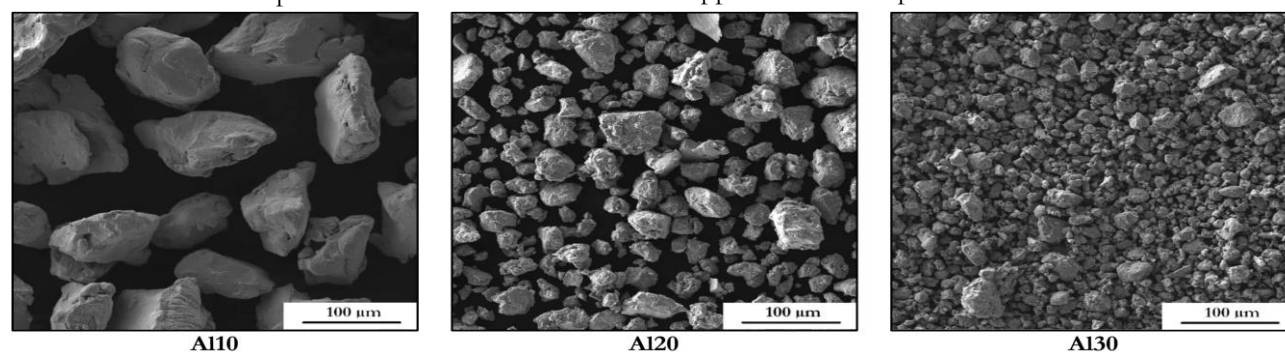


**Fig. 1** *Morphology of the CoCrFeNiAlX alloy powders as a consequence of Al content after mechanical alloying for 8 h*

The microstructure of MA+SPS compacts is shown in Figure 2. One can see, that the microstructure of the CoCrFeNiAlX high-entropy alloys is in all cases ultrafine-grained and becomes even finer with increasing content of Al. This is in good agreement with the results of others [11,15,16], and also corresponds to the powder's morphology (see Fig. 1) that pointed to such presumptions. Another thing that we can observe from Fig. 2 is pores manifest themselves as dark points. It is visible

that each sample has a certain number of pores which average percentage decreases with increasing Al content. Moreover, the Al30 showed strong dissolving of the grain boundaries which could be mistaken for insufficient sintering of the sample. However, accordingly to the XRD results, the main reason might be an increasing content of the phase with primitive centered (PC) crystallographic lattice identified as  $\text{Al}(\text{Co}_{0.5}\text{Ni}_{0.5})$  which might be easily dissolved during the etching.

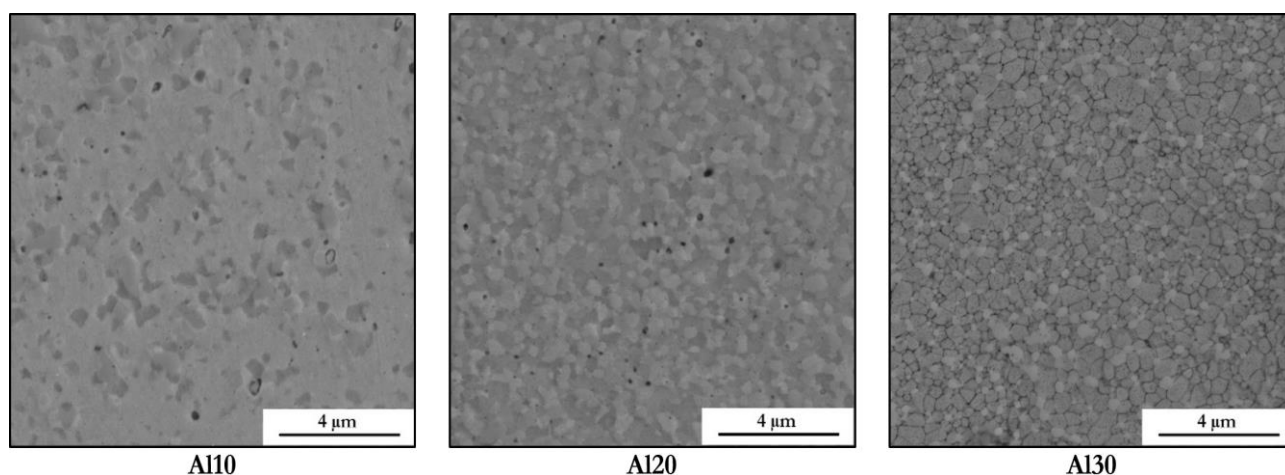


**Fig. 2** SEM micrographs of the MA+SPS CoCrFeNiAlX alloys

The results of the XRF analysis are shown in Table 2. It is visible that with the Al content increases, other elements' content decreases. It is in good agreement with the theoretical weights of the initial powders which were used for the preparation of the CoCrFeNiAlX alloys (Table 1). It is interesting

that at the beginning of the study there wasn't presence of Si in the high-entropy alloys. Its presence can be described by cleaning the grinding vessel and grinding media with SiC. To prevent this contamination, the grinding things must be more carefully cleaned.

**Tab. 2** Chemical composition of the CoCrFeNiAlX alloy according to XRF analysis

	element content, at. %					
	Co	Cr	Fe	Ni	Al	Si
<b>Al10</b>	21.5	22.0	23.5	23.0	8.5	1.5
<b>Al20</b>	19.2	18.1	22.1	21.4	16.2	2.9
<b>Al30</b>	15.9	16.3	25.0	18.1	23.1	1.0

To better understand why the microstructure of the studied high-entropy alloy changed with a different Al content, the XRD analysis was done. The results of the phase composition of the individual alloys are shown in Figure 3. One can see that the Al10 alloy shows the three highest peaks which were identified as the ductile FCC solid solution corresponding to a  $\text{Cr}_{0.25}\text{Fe}_{0.25}\text{Co}_{0.25}\text{Ni}_{0.25}$  phase. Nonetheless, there were also peaks corresponding to BCC solid solution which were identified as  $\alpha$ -Fe and some minor fraction of  $\text{Al}(\text{Co}_{0.5}\text{Ni}_{0.5})$  phase with PC crystallographic lattice. On the contrary, the increase of the Al content in the alloy caused the annihilation of the FCC solid solution at the expense of the PC crystallographic lattice formation. The content of the

$\alpha$ -Fe and the  $\text{Al}(\text{Co}_{0.5}\text{Ni}_{0.5})$  phases increased reaching the highest intensities in the case of Al30 alloy. Moreover, the peaks showed some microstructure-related effects reducing its FWHM values with increasing content of Al supporting the already mentioned microstructural refinement as the Al content increases. Among that, the formation of two carbides ( $\text{Cr}_7\text{C}_3$  and  $\text{Cr}_{23}\text{C}_6$ ) was observed. The present carbide particles tend to form during the SPS compaction as the powders are supersaturated with C as a consequence of n-heptane used during the MA. Accordingly, to the [18], the form of the carbides is related to the content of C within the carbide forming the  $\text{Cr}_{23}\text{C}_6$  (15-20% C),  $\text{Cr}_7\text{C}_3$  (20-30% C), or  $\text{Cr}_3\text{C}_2$  (30-45% C).

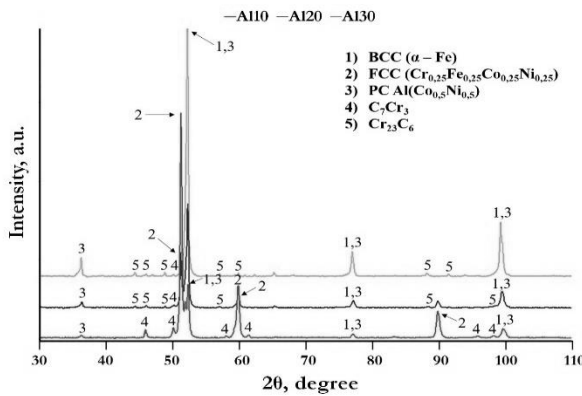


**Fig. 3** XRD patterns of CoCrFeNiAlX alloys after the SPS process

**Tab. 3** Phase composition of the studied CoCrFeNiAlX alloys as a consequent of the Al content

	SemiQuant, %				
	BCC ( $\alpha$ -Fe)	FCC ( $\text{Cr}_{0.25}\text{Fe}_{0.25}\text{Co}_{0.25}\text{Ni}_{0.25}$ )	PC Al( $\text{C}_{0.5}\text{Ni}_{0.5}$ )	$\text{Cr}_7\text{C}_3$	$\text{Cr}_{23}\text{C}_6$
Al10	15	58	7	20	
Al20	32	18	22	22	6
Al30	52		30		18

### 3.2 Mechanical properties

Figure 4 shows the relationship between porosity and the hardness of the high-entropy CoCrFeNiAlX alloys. It is visible that with the increasing Al content the porosity reduces while the hardness contrarily increases. One can see that the best results have been obtained in the Al30 alloy reaching a hardness of approximately 732 HV 30. This is a result of having higher volume content of both the BCC and PC phases compared to the other alloys. On the other hand, the volume fraction of the  $\text{Cr}_{23}\text{C}_6$  carbide is more or less the same as the content of  $\text{Cr}_7\text{C}_3$ . In the work of others [19], the hardness of carbides was calculated to be 1377 HV ( $\text{Cr}_7\text{C}_3$ ) and 1030 HV ( $\text{Cr}_{23}\text{C}_6$ ). Therefore, the resulting hardness increase is truly caused by the content of the BCC and PC phases while the phase swap of  $\text{Cr}_7\text{C}_3$  into softer  $\text{Cr}_{23}\text{C}_6$  is acting contrarily. The surface porosity of the samples was showing the opposite trend reaching the highest porosity in the case of the Al10 alloy. This can be related to the internal porosity of the powders themselves, which might be higher in the case of coarser microstructure and was retained even after the SPS compaction. On the other hand, in the case of Al30 alloy, the present pores are acting as stress-concentrators promoting the recurring fragmentation of the powder particles resulting in a significant microstructural refinement. Such presumption is in good agreement with the other results [4,20], of the compressive stress-strain tests which showed a transition from a ductile into a brittle behaviour with increasing content of Al. More importantly, this is also further supported by the commonly observed fact, that materials with higher hardness (and also

The volume percentage of the identified phases is shown in Table 3. It is clearly visible that increasing the content of Al to 20 at.% reduced the volume fraction of ductile FCC phase to less than a third of the original value newly achieving only 18 %. Considering the results of the XRD analysis one can say that the refinement of the powder particles is caused by the increasing content of the BCC phase. The results correspond with results from other researchers [12,15,17] that described the same effect of the Al on the transformation from FCC to BCC. Phase composition changes can also positively affect the mechanical properties (below).

brittleness) are usually showing higher porosity after the SPS compaction due to difficult interparticle cohesions [20]. Concerning Fig. 2 and Fig. 4 one can say that the best properties have the high-entropy alloy CoCrFeNiAlX with 20 at.% of Al.

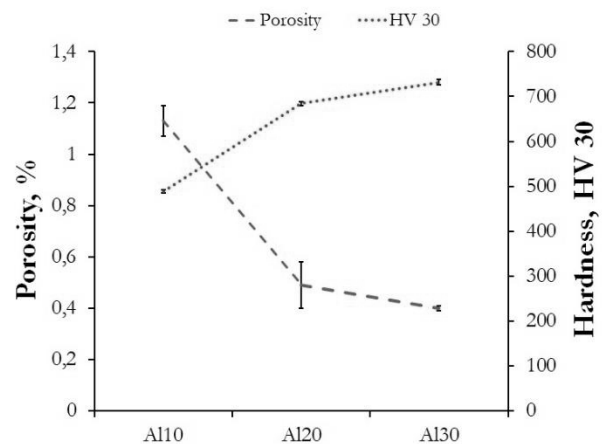


**Fig. 4** Hardness HV 30 and porosity of compacted CoCrFeNiAlX alloy depending on Al content

To confirm the last statement, compression tests at laboratory temperature were done for all studied CoCrFeNiAlX alloys. The results of the tests are shown in Figure 5. One can see that increasing the Al content in the HEA reduced the ductility transforming the formerly ductile materials into a much more brittle ones. The statement is in good relation with the results of the XRD analysis (see Fig. 3) confirming the increasing content of BCC+PC phases at the expense of ducting FCC. The alloy with 10 at.% of Al has the highest ductility, but the lowest ultimate compressive strength (UCS) and compressive yield strength (CYS).



The Al30 alloy showed almost negligible ductility being able to reach the UCS of 2300 MPa. The best results were achieved in the case of Al20 alloy that retained certain ductility having CYS of  $2066 \pm 28$  MPa while reaching the highest UCS of  $2470 \pm 37$  MPa among all the tested alloys. The main reason was the coexistence of ductile FCC solid solution within the structure of such material.

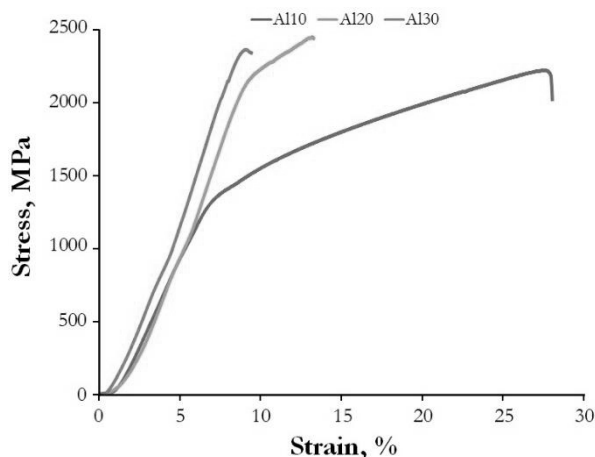


**Fig. 5** Compression stress-strain curves of the compacted CoCrFeNiAlX alloys show the influence of Al content on overall behaviour

#### 4 Conclusions

In the work, the change of microstructure and mechanical properties of the mechanically alloyed high-entropy CoCrFeNiAlX alloy as a result of Al content was described. It was found that microstructure becomes finer and materials porosity reduces with the increase of the Al content. The XRD analysis revealed, that the amount of both the solid solutions with BCC and FCC crystallographic lattice changed favouring the existence of a BCC solid solution accompanied by a phase identified as  $\text{Al}(\text{Co}_{0.5}\text{Ni}_{0.5})$  with PC lattice. This resulted in the improvement of mechanical properties reaching the maximal UCS in the case of Al20 alloy, which also retained some ductility. This alloy achieved the best combination of microstructure and mechanical properties values. The highest hardness was achieved in the case of Al30 alloy, which was showing a rather brittle behaviour due to the absence of FCC solid solution.

#### Acknowledgment

*The research was financially supported by Czech Science Foundation (grant No. 21-11313S).*

#### References

- [1] YEH, J.W., et al. (2004). Nanostructured high-entropy alloys with multiple principal elements: novel alloy design concepts and outcomes. *Advanced Engineering Materials*. Vol. 6, No. 5, pp. 299-303
- [2] CANTOR, B., et al. (2004). Microstructural development in equiatomic multicomponent alloys. *Materials Science and Engineering: A*. 375-377: pp. 213-218
- [3] GUO, S. (2015). Phase selection rules for cast high entropy alloys: an overview. *Materials Science and Technology*. Vol.31, No.10, pp. 1223-1230
- [4] VESELKA Z., PRŮŠA, F., ŠENKOVÁ, A., VOJTĚCH, D. (2020). Slitiny s vysokou entropií - historie, příprava, vlastnosti a výzkum. *Chemické listy*, p. 114
- [5] ZHANG, Y., et al. (2014). Microstructures and properties of high-entropy alloys. *Progress in Materials Science*. 61, pp. 1-93
- [6] GAO, M.C., et al. (2016). High-Entropy Alloys: Fundamentals and Applications: Fundamentals and Applications. Cham, SWITZERLAND: Springer International Publishing AG
- [7] YANG, X., CHEN, S.Y., COTTON, J.D., et al. (2014). Phase Stability of Low-Density, Multiprincipal Component Alloys Containing Aluminum, Magnesium, and Lithium. *JOM*. 66, pp. 2009-2020
- [8] VAIDYA, M., MURALIKRISHNA, G.M., and MURTY, B.S. (2019). High-entropy alloys by mechanical alloying: A review. *Journal of Materials Research*. Vol. 34, No. 5, pp. 664-686
- [9] PINC, J., ŠKOLÁKOVÁ, A., VEŘTÁT, P., ČAPEK, J., ŽOFKOVÁ, Z., RIESZOVÁ, L., HABR, S. & VOJTĚCH, D. 2020. Microstructural characterization and optimization of the  $\text{ZnMg}_{0.8}(\text{CaO})_{0.26}$  alloy processed by ball milling and subsequent extrusion. *Manufacturing Technology*, 20, 484-91
- [10] TORRALBA, J.M., ALVAREDO, P., and GARCÍA-JUNCEDA, A. (2019). High-entropy alloys fabricated via powder metallurgy. A critical review. *Powder Metallurgy*. Vol. 62, No. 2, pp. 84-114
- [11] WANG, W.-R., WANG, W.-L., WANG, S.-C., TSAI, Y.-C., LAI, C.-H., & YEH, J.-W. (2012). Effects of Al addition on the microstructure and mechanical property of  $\text{AlxCoCrFeNi}$  high-entropy alloys. *Intermetallics*. 26, pp. 44-51
- [12] YANG, T., XIA, S., LIU, S., WANG, C., LIU, S., ZHANG, Y., WANG, Y. (2015). Effects of AL addition on microstructure and mechanical properties of  $\text{AlxCoCrFeNi}$  High-entropy

- alloy. *Materials Science and Engineering: A*. 648, pp. 15-22
- [13] CAO, T., SHANG, J., ZHAO, J., CHENG, C., WANG, R., & WANG, H. (2016). The influence of Al elements on the structure and the creep behavior of AlxCoCrFeNi high entropy alloys. *Materials Letters*. 164, pp. 344-347
- [14] KAO, Y.F., CHEN, S.K., CHEN, T.J., CHU, P.C., YEH, J.W., & LIN, S.J. (2011). Electrical, magnetic, and Hall properties of AlxCoCrFeNi high-entropy alloys. *Journal of Alloys and Compounds*. Vol. 509, No. 5, pp. 1607-1614
- [15] WANG, W.R., WANG, W.L., & YEH, J.W. (2014). Phases, microstructure and mechanical properties of AlxCoCrFeNi high-entropy alloys at elevated temperatures. *Journal of Alloys and Compounds*. 589, pp. 143-152
- [16] SHI, Y., COLLINS, L., FENG, R., ZHANG, C., BALKE, N., LIAW, P. K., & YANG, B. (2018). Homogenization of AlxCoCrFeNi high-entropy alloys with improved corrosion resistance. *Corrosion Science*. 133, pp. 120-131
- [17] GARLAPATI, M.M., et al. (2020). Influence of Al content on thermal stability of nanocrystalline AlxCoCrFeNi high entropy alloys at low and intermediate temperatures. *Advanced Powder Technology*. Vol. 31, No. 5, pp. 1985-1993
- [18] GANGULY, A., MURTHY, V., & KANNOORPATTI, K. (2020). Structural and electronic properties of chromium carbides and Fe-substituted chromium carbides. *Materials Research Express*. Vol. 7, No. 5
- [19] SUN, L., JI, X., ZHAO, L., ZHAI, W., XU, L., DONG, H., LIU, Y., PENG, J. (2022). First Principles Investigation of Binary Chromium Carbides Cr<sub>7</sub>C<sub>3</sub>, Cr<sub>3</sub>C<sub>2</sub> and Cr<sub>23</sub>C<sub>6</sub>: Electronic Structures, Mechanical Properties and Thermodynamic Properties under Pressure. *Materials*. Vol. 15, No. 2, p. 558
- [20] THÜRLOVÁ, H. & PRŮŠA, F. 2022. Partial Substitution of Mn by Al in the CoCrFeNiMn<sub>x</sub>Al<sub>20-x</sub> (X=5, 10, 15) High Entropy Alloy Prepared of Mechanical Alloying and Spark Plasma Sintering. *Manufacturing Technology*, 22, 342-6